

# Measurement of the rate coefficient for the OH + NO<sub>2</sub> reaction under the atmospheric pressure: Its humidity dependence

Y. Sadanaga<sup>a,b,\*</sup>, S. Kondo<sup>c</sup>, K. Hashimoto<sup>c</sup>, Y. Kajii<sup>a,\*</sup>

<sup>a</sup> Department of Applied Chemistry, Graduate School of Engineering, Tokyo Metropolitan University, 1-1 Minami-Osawa, Hachioji, Tokyo 192-0397, Japan

<sup>b</sup> Japan Science and Technology Agency, 4-1-8, Honcho, Kawaguchi, Saitama 332-0012, Japan

<sup>c</sup> Department of Chemistry, Graduate School of Science, Tokyo Metropolitan University, 1-1 Minami-Osawa, Hachioji, Tokyo 192-0397, Japan

Received 29 August 2005; in final form 2 December 2005

Available online 4 January 2006

## Abstract

Humidity dependence of the rate coefficient of the OH + NO<sub>2</sub> reaction has been studied. The rate coefficients, measured at the H<sub>2</sub>O partial pressures ( $P_{\text{H}_2\text{O}}$ ) of 29.1 and 3.7 hPa and at 298 K are  $(1.15 \pm 0.02) \times 10^{-11}$  and  $(1.40 \pm 0.10) \times 10^{-11}$  cm<sup>3</sup> molecule<sup>-1</sup> s<sup>-1</sup> ( $\pm 2\sigma$ ), respectively. The equilibrium constant of the NO<sub>2</sub>–H<sub>2</sub>O system estimated using ab initio calculations is too small to explain the retardation of the reaction under our experimental conditions. Thus, we conclude that the NO<sub>2</sub>–H<sub>2</sub>O cannot contribute significantly to the OH + NO<sub>2</sub> reaction in the atmosphere near the ground surface.

© 2005 Elsevier B.V. All rights reserved.

## 1. Introduction

The reaction of OH with NO<sub>2</sub> is one of the most important processes in the troposphere for two reasons: First, this reaction produces nitric acid (HNO<sub>3</sub>) and contributes to acidification of the Earth's environment.



Second, this reaction is a main chain-termination step of the oxidation cycles involving HO<sub>x</sub> (=OH and HO<sub>2</sub>) and NO<sub>x</sub> (=NO and NO<sub>2</sub>) radicals. This is because both HO<sub>x</sub> and NO<sub>x</sub> are removed via this reaction from the atmosphere. In spite of numerous investigations on the kinetics of this reaction at various pressures and temperatures (see e.g. [1–6]), its rate coefficients are still controversial, and the recommended values have large uncertainties.

Recently, a new mechanism has been proposed for this reaction. Namely, a reversible reaction also proceeds to produce a significant amount of pernitrous acid, HOONO [7].



A recent spectroscopic experiment has demonstrated the existence of HOONO [8]. This branching reaction has been speculated to be one of the reasons for the uncertainties in the recommended rate coefficients. Another reason is that only few reliable measurements have yet been made on the rate coefficient of this reaction under atmospheric conditions [6].

In the present study, we have measured the rate coefficient of the OH + NO<sub>2</sub> reaction under ambient conditions, especially the dependence on humidity. To the best of our knowledge, this is the first measurement of the humidity dependence under ambient conditions.

## 2. Experimental

The rate constant was measured by the use of a combined technique of laser flash photolysis/laser-induced fluorescence. Fig. 1 shows a schematic diagram of the

\* Corresponding authors. Present address: Department of Applied Chemistry, Graduate School Engineering, Osaka Prefecture University, 1-1 Gakuen-cho, Sakai, Osaka 599-8531, Japan (Y. Sadanaga). Fax: +81 72 254 9326 (Y. Sadanaga), +81 426 77 2837 (Y. Kajii).

E-mail addresses: [sadanaga@chem.osakafu-u.ac.jp](mailto:sadanaga@chem.osakafu-u.ac.jp) (Y. Sadanaga), [kajii@atmchem.apchem.metro-u.ac.jp](mailto:kajii@atmchem.apchem.metro-u.ac.jp) (Y. Kajii).

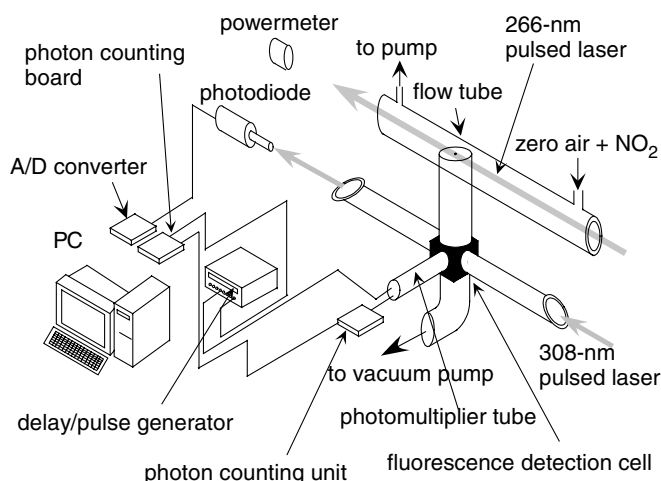
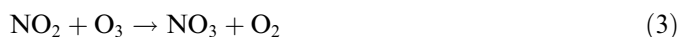


Fig. 1. Schematic drawing of the experimental apparatus.

experimental apparatus, described in detail in Refs. [9,10]. All the experiments were conducted at 298 K.

The sample of NO/N<sub>2</sub> gas (5.16 ppmv, Nippon Sanso, ppmv: parts per million by volume) was diluted by zero-air, and the total NO/air flow was controlled to be 500 sccm (standard cubic centimeters per minute). The NO concentrations of the NO/air mixture were controlled to range from 1 to 5 ppmv. The NO/air gas was mixed with O<sub>3</sub>/zero-air mixture (≈250 ppmv of O<sub>3</sub>) to generate NO<sub>2</sub>. The flow rate of the mixture ranged up to 20 sccm, depending on the NO concentration in the NO/air mixture. Zero-air was generated by passing compressed ambient air through a hot Pt oven (623 K) and purafil-charcoal filters to remove most of the OH reaction partners. In zero-air, the concentrations of CO, NO<sub>x</sub> and hydrocarbons were less than 10 ppbv (parts per billion by volume), 50 and 10 pptv (parts per trillion by volume), respectively. O<sub>3</sub> was produced in the photolysis of O<sub>2</sub> in zero-air using a low-pressure mercury lamp (SP-5-2H, Sen light).

The reaction time of NO with O<sub>3</sub> was controlled to convert NO to NO<sub>2</sub> entirely, and to avoid generations of NO<sub>3</sub> and N<sub>2</sub>O<sub>5</sub> via subsequent reactions.



Typically, the reaction time was set to 3 s. These concentrations were estimated by box model calculations, which indicated that the concentrations of N<sub>2</sub>O<sub>5</sub> and NO<sub>3</sub> were 2 and 5 orders of magnitude smaller than that of NO<sub>2</sub>, respectively. Therefore, the interferences of NO<sub>3</sub> and N<sub>2</sub>O<sub>5</sub> are negligible, in comparison with the rate constants for the reactions of OH with these species. In addition, the actual NO<sub>3</sub> and N<sub>2</sub>O<sub>5</sub> concentrations should be even smaller than these estimates, because the wall loss of NO<sub>3</sub> was ignored in these calculations. Similar results were obtained for the other concentrations of initial NO (1–5 ppmv).

The NO<sub>2</sub>/O<sub>3</sub> mixture was diluted with a large flow (≈25 L min<sup>-1</sup>) of zero-air. Residual NO was found to be negligible by a measurement using an O<sub>3</sub> chemilumines-

cence detector (Model 42S, Thermo Electron). To study the humidity dependence of the OH + NO<sub>2</sub> rate coefficient, the humidity of zero-air was controlled. A part of the flow was divided, bubbled through a trap of distilled water and then returned to the main flow. The humidity of the NO<sub>2</sub>/zero-air mixture, monitored by a sensor (Shinyei, THPCA9), was found to be constant within ±3% RH (relative humidity) during the experiment. The H<sub>2</sub>O partial pressure during the experiment ranged from 4 to 29 hPa.

The NO<sub>2</sub>/O<sub>3</sub>/H<sub>2</sub>O/zero-air mixture was introduced into a flow tube. The pressure in the flow tube was approximately 990 hPa, as measured using a capacitance manometer (Baratron model 626A, MKS). A fourth harmonic of a Nd:YAG laser (Quanta-Ray INDI-40, Spectra-Physics) with a low repetition rate (1 or 2 Hz) was irradiated to generate OH radicals.



The OH radical reacted with NO<sub>2</sub> in the flow tube, and the concentration of OH declined after the irradiation of the 266-nm laser pulse. The decay of the OH concentration after the 266-nm laser pulse was measured by the time-resolved LIF technique. OH was excited at 308 nm using a tunable frequency-doubled dye laser (Scanmate, Lambda Physik) pumped by a frequency-doubled Nd:YVO<sub>4</sub> laser with a repetition rate of 10 kHz (YHP40-532Q, Spectra-Physics). The resonant fluorescence was detected using a dynode-gated photomultiplier tube (R2256P, Hamamatsu). The interval of pulse trains of the 308-nm laser (corresponding to 100 μs) was used as a clock for the measurement of the OH decay rates.

The NO<sub>2</sub> concentration in the flow tube was measured using the LIF technique [11,12]. Since NO<sub>2</sub> sensitivity decreases with humidity, due to the fast quenching of the excited NO<sub>2</sub> by H<sub>2</sub>O, the NO<sub>2</sub> measurement system was calibrated, including consideration of H<sub>2</sub>O quenching [11].

The first-order decay rate of the OH radical was measured by varying the NO<sub>2</sub> concentrations under the same humidity conditions. Fig. 2 shows an example of the measured OH decay profile by the reaction of OH with NO<sub>2</sub> in logarithmic scale. The time series of OH signals shows two decay components. The slower decay reflects the OH + NO<sub>2</sub> reaction, OH diffusion and turbulence in the flow tube. The fast decay can be attributed to rapid diffusion of OH radicals by the ‘local’ 266-nm laser irradiation, where ‘local’ means that the diameter of the 266-nm laser beam, 10 mm, is smaller than the inner diameter of the flow tube, 40 mm. In other words, the OH radical is first generated within the 10 mm center circuit of the flow tube by the laser irradiation and then OH diffuses toward the inner wall of the flow tube. When the 266 nm laser was irradiated ≈15 mm upside of the radial center of the flow tube, no fast decay was observed but the rise of the LIF signal slowed down (corresponding to the timescale of the fast decay). This indicates that no OH radical is first generated at the

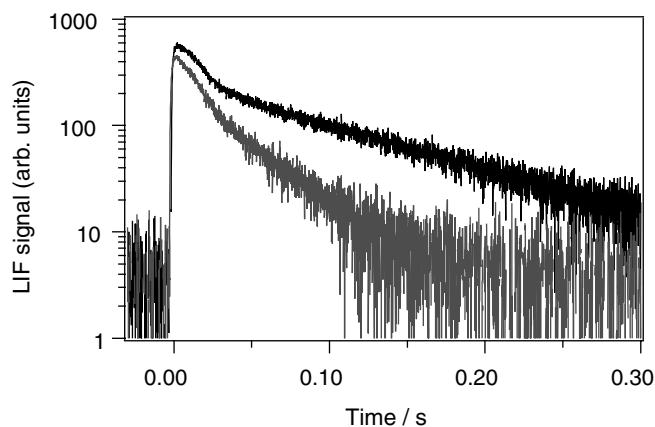


Fig. 2. Examples of the measured OH decay profile by the reaction of OH with  $\text{NO}_2$  in logarithmic scale. Black line:  $[\text{NO}_2] = 5.61 \times 10^{11}$  molecules  $\text{cm}^{-3}$ . Gray line:  $[\text{NO}_2] = 1.68 \times 10^{12}$  molecules  $\text{cm}^{-3}$ .

center of the flow tube (i.e., inlet of the fluorescence detection cell) and then OH diffuses toward the inlet of the fluorescence detection cell. A previous measurement of the rate coefficient of the OH + CO reaction demonstrated the accuracy of this instrument [9]. The decay profiles were analyzed by the following fitting equation, in which the slower decay component was taken into account.

$$[\text{OH}] = [\text{OH}]_0 \exp(-k'_{\text{NO}_2} t) \quad (7)$$

The measured decay rates in the presence of  $\text{NO}_2$  ( $k'_{\text{NO}_2}$ ) and in zero-air ( $k'_{\text{zero}}$ ) were measured alternately to confirm the zero point of the decay rate.

### 3. Results and discussion

#### 3.1. Humidity dependence of the rate coefficient

Kinetic measurements were conducted under pseudo-first-order conditions. The initial OH concentrations were  $\approx 10^9$  radicals  $\text{cm}^{-3}$ . The concentrations of  $\text{NO}_2$  ranged from  $3 \times 10^{11}$  to  $3 \times 10^{12}$  molecules  $\text{cm}^{-3}$ . The contribution of  $\text{N}_2\text{O}_4$  via the following equilibrium can be neglected because of its small equilibrium constant ( $2.8 \times 10^{-19}$  molecules $^{-1}$   $\text{cm}^3$  at 298 K [13]).



Fig. 3 shows an example of the measured first-order rate coefficients for the reaction of OH with  $\text{NO}_2$  as a function of the  $\text{NO}_2$  number density. The solid line in Fig. 2 shows the weighted linear least-squares fit to the data. The slope of the regression line gives the second-order rate coefficient. Fig. 4 represents the humidity dependence of the second-order rate coefficient. At the  $\text{H}_2\text{O}$  partial pressure ( $P_{\text{H}_2\text{O}}$ ) of 3.7 hPa, the rate coefficient was found to be  $(1.40 \pm 0.10) \times 10^{-11}$   $\text{cm}^3$  molecule $^{-1}$   $\text{s}^{-1}$ , which is in excellent agreement with the IUPAC1997 recommended value [14]. However, this coefficient decreased with the  $\text{H}_2\text{O}$  concentration to  $(1.15 \pm 0.02) \times 10^{-11}$   $\text{cm}^3$  molecule $^{-1}$   $\text{s}^{-1}$  at 29.1 hPa. The main uncertainty,  $\pm 2\sigma$ , in this coefficient,

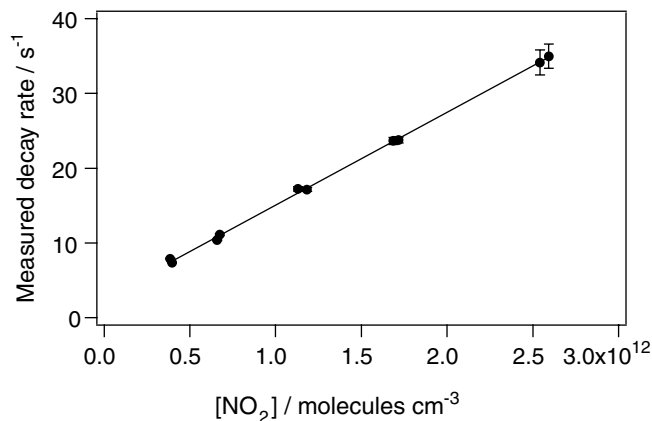


Fig. 3. Plots of measured first-order decay rate ( $k'_{\text{NO}_2}$ ) versus  $\text{NO}_2$  concentrations at 745 Torr total air pressure and at 298 K. Solid line shows linear regression lines. Its slope gives the second-order decay rate constant of  $(1.21 \pm 0.03) \times 10^{-11}$   $\text{cm}^3$  molecule $^{-1}$   $\text{s}^{-1}$ . The error bars, representing  $\pm 2\sigma$ , for the number densities fall within the circles except in the extreme end.

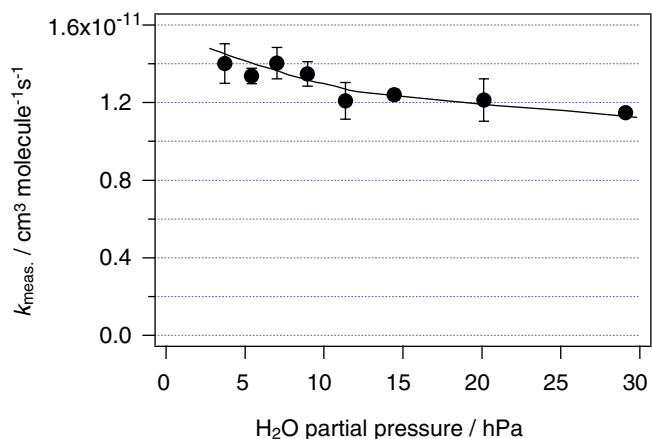


Fig. 4. The measured second-order rate coefficients for the OH +  $\text{NO}_2$  reaction as a function of the partial pressure of water vapor at 298 K. The total pressure in the reaction tube was measured to be 745 Torr in air condition. Error bars show  $\pm 2\sigma$ . A solid line is a just guide to the eyes.

where  $\sigma$  stands for standard error, arises from the measurements of the OH decay rate ( $\pm 15\%$ ) [9] and the  $\text{NO}_2$  concentration ( $\pm 5\%$ ). Considering these uncertainties, we conclude that the observed decrease in the rate coefficient is significant.

#### 3.2. Possibility of OH– $\text{H}_2\text{O}$ and $\text{NO}_2$ – $\text{H}_2\text{O}$ complexes formation as a cause of the slowdown of the reaction

Our results indicate that the rate coefficient for the OH +  $\text{NO}_2$  reaction decreases in the presence of water vapor. One may suspect that molecular complexes, such as OH– $\text{H}_2\text{O}$  and  $\text{NO}_2$ – $\text{H}_2\text{O}$  play some role in the slowdown of the reaction. The structures of four relevant complexes, shown in Fig. 5, were optimized at the B3LYP/aug-cc-pVTZ level using the GAUSSIAN03 program [15]. In the most stable structure of OH– $\text{H}_2\text{O}$ , the OH radical acts

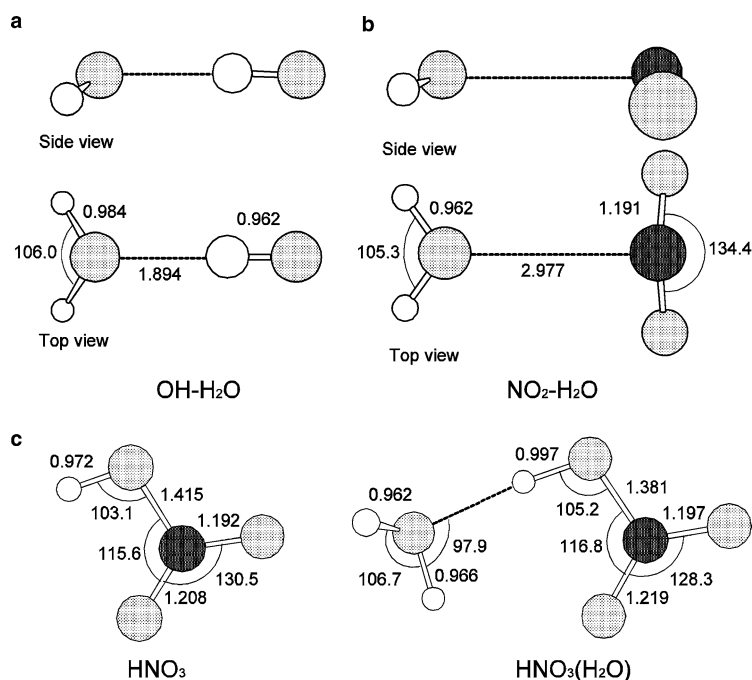


Fig. 5. Optimized geometries of: (a) OH-H<sub>2</sub>O, (b) NO<sub>2</sub>-H<sub>2</sub>O, and (c) HNO<sub>3</sub> and HNO<sub>3</sub>(H<sub>2</sub>O) at the B3LYP/aug-cc-pVTZ level. Geometric parameters are given in angstroms and degrees.

as a proton donor, in agreement with a recent experimental observation [16]. The calculated binding energy is  $-3.2$  kcal/mol with both counterpoise correction (CPC) [17] for the basis set superposition error (BSSE) and zero-point correction (ZPC). On the other hand, the binding energy of NO<sub>2</sub>-H<sub>2</sub>O, where the H<sub>2</sub>O molecule is bound to N by the O atom, is  $-0.50$  kcal/mol with CPC and ZPC. Neither reaction, OH-H<sub>2</sub>O + NO<sub>2</sub> → HNO<sub>3</sub>(H<sub>2</sub>O) or OH + NO<sub>2</sub>-H<sub>2</sub>O → HNO<sub>3</sub>(H<sub>2</sub>O), indicates a potential barrier, suggesting that the appearance of the barrier is not responsible for the slow reaction in the presence of the water. So, the water may interfere with the collision between OH and NO<sub>2</sub> resulting in the reduced reaction cross section, though further effort at the molecular level is necessary to unveil the reason for the retardation of the reaction by the water.

The equilibrium constant,  $K_P$ , or the abundance of the complexes, is informative to assess their contribution to the reaction under our experimental conditions. It is difficult at present to evaluate the  $K_P$  for OH + H<sub>2</sub>O ↔ OH-H<sub>2</sub>O, mainly because there is a low-lying electronic excited state [16]. Thus, we focused on the abundance of the NO<sub>2</sub>-H<sub>2</sub>O complex relative to the free NO<sub>2</sub> molecule. The ratio of the partial pressure of NO<sub>2</sub>-H<sub>2</sub>O,  $P_{\text{NO}_2\text{-H}_2\text{O}}$ , over that of free NO<sub>2</sub>,  $P_{\text{NO}_2}$ , was estimated using the following formula,

$$\frac{P_{\text{NO}_2\text{-H}_2\text{O}}}{P_{\text{NO}_2}} = \frac{\left(\frac{P_{\text{NO}_2\text{-H}_2\text{O}}}{P}\right)}{\left(\frac{P_{\text{NO}_2}}{P}\right)} = K_P P \left(\frac{P_{\text{H}_2\text{O}}}{P}\right), \quad (9)$$

where  $K_P$  is the equilibrium constant of NO<sub>2</sub>-H<sub>2</sub>O, while  $P_{\text{H}_2\text{O}}$  and  $P$  are the partial pressures of water and the atmospheric pressure, respectively.  $K_P$ , which is a function of

temperature, can be evaluated using the partition functions of the complex and monomers within the rigid rotator approximation. The rotational constants, harmonic frequencies and binding energies at the B3LYP/aug-cc-pVTZ level were used for the calculations of the partition functions. The translational and rotational partition functions were computed using textbook formulas [18]. For calculation of the vibrational partition function for the complex, the levels below the dissociation energy were included straightforwardly, and thus, a total of 29 states were used [19]. Total pressure,  $P$ , and temperature,  $T$ , were set to 990 hPa and 298 K, respectively. The calculated  $K_P$  was  $1.52 \times 10^{-5}$  bar<sup>-1</sup>, while the ratio  $P_{\text{NO}_2\text{-H}_2\text{O}}/P_{\text{NO}_2}$  was  $5.62 \times 10^{-8}$  and  $4.42 \times 10^{-7}$  when the  $P_{\text{H}_2\text{O}}$  values were 3.7 and 29.1 hPa, respectively. The values of  $P$ ,  $T$  and  $P_{\text{H}_2\text{O}}/P$  employed are close to the standard values for the mid-latitudes [20]. Since the intermolecular harmonic frequencies at the present level are known to be usually overestimated, giving rise to lower density of states, the calculated  $K_P$  may be slightly below the actual value [19]. Nevertheless, the order of the magnitude of the  $P_{\text{NO}_2\text{-H}_2\text{O}}/P_{\text{NO}_2}$  based on our  $K_P$  is deemed to be so small that the NO<sub>2</sub>-H<sub>2</sub>O cannot contribute significantly to the OH + NO<sub>2</sub> reaction under our conditions, namely, in the atmosphere near the ground surface.

#### Acknowledgments

The authors are grateful to our colleagues (A. Yoshino, K. Watanabe, A. Yoshioka, N. Akiyama, A. Nishiyama and J. Matsumoto) for their assistance in the  $k_{\text{NO}_2}$  measurements. This work was supported financially by Core

Research for Evolutional Science and Technology (CREST) from Japan Science and Technology Agency, and by the Ministry of Education, Science, Sports and Culture of Japan (Grant-in-Aid No. 15201004).

## References

- [1] R. Forster, M. Frost, D. Fulle, H.F. Hamann, H. Hippler, A. Schlegel, J. Troe, *J. Chem. Phys.* 103 (1995) 2949.
- [2] N.M. Donahue, M.K. Dubey, R. Mohrschladt, K.L. Demerjian, J.G. Anderson, *J. Geophys. Res.* 102 (1997) 6159.
- [3] D. Fulle, H.F. Hamann, H. Hippler, J. Troe, *J. Chem. Phys.* 108 (1998) 5391.
- [4] T.J. Dransfield, K.K. Perkins, N.M. Donahue, J.G. Anderson, M.M. Sprengnether, K.L. Demerjian, *Geophys. Res. Lett.* 26 (1999) 687.
- [5] S.S. Brown, R.K. Talukdar, A.R. Ravishankara, *Chem. Phys. Lett.* 299 (1999) 277.
- [6] L. D'Ottone, P. Campuzano-Jost, D. Bauer, A.J. Hynes, *J. Phys. Chem. A* 105 (2001) 10538.
- [7] D.M. Golden, G.P. Smith, *J. Phys. Chem. A* 104 (2000) 3991.
- [8] S.A. Nizkorodov, P.O. Wennberg, *J. Phys. Chem. A* 106 (2002) 855.
- [9] Y. Sadanaga, A. Yoshino, K. Watanabe, A. Yoshioka, Y. Wakazono, Y. Kanaya, Y. Kajii, *Rev. Sci. Instrum.* 75 (2004) 2648.
- [10] Y. Sadanaga, A. Yoshino, S. Kato, A. Yoshioka, K. Watanabe, Y. Miyakawa, I. Hayashi, M. Ichikawa, J. Matsumoto, A. Nishiyama, N. Akiyama, Y. Kanaya, Y. Kajii, *Geophys. Res. Lett.* 31 (2004) L08102, doi:10.1029/2004GL019661.
- [11] J. Matsumoto, J. Hirokawa, H. Akimoto, Y. Kajii, *Atmos. Environ.* 35 (2001) 2803.
- [12] J. Matsumoto, Y. Kajii, *Atmos. Environ.* 37 (2003) 4847.
- [13] S.P. Sander et al., *JPL Publ.* 02–25 2002.
- [14] R. Atkinson, D.L. Baulch, R.A. Cox, R.F. Hampson Jr., J.A. Kerr, M.J. Rossi, J. Troe, *J. Phys. Chem. Ref. Data* 26 (1997) 1329.
- [15] M.J. Frisch et al., *Gaussian Suite GAUSSIAN 03, Revision B.03*, Gaussian Inc., Pittsburgh, PA, 2003.
- [16] Y. Ohshima, K. Sato, Y. Sumiyoshi, Y. Endo, *J. Am. Chem. Soc.* 127 (2005) 1108.
- [17] S.F. Boyds, F. Bernardi, *Mol. Phys.* 19 (1970) 553.
- [18] D.A. McQuarrie, J.D. Simon, *Physical Chemistry. A Molecular Approach*, University Science Books, Sausalito, CA, 1997.
- [19] A. Sabu, S. Kondo, R. Saito, Y. Kasai, K. Hashimoto, *J. Phys. Chem. A* 109 (2005) 1836.
- [20] G. Brasseur, S. Solomon, *Aeronomy of the Middle Atmosphere*, second edn., D. Reidel, Dordrecht, The Netherlands, 1986.